

# Effect of the size of the central atom on the stability of crystalline phases in solid solutions $(\text{NH}_4)_3\text{Ti}_x\text{Sn}_{1-x}\text{F}_7$

Evgeniy V. Bogdanov<sup>a,b,c,\*</sup>, Evgeniy I. Pogoreltsev<sup>a,c</sup>, Mikhail V. Gorev<sup>a,c</sup>,  
Svetlana V. Mel'nikova<sup>a</sup>, Maxim S. Molokeev<sup>a,c</sup>, Natalia M. Laptash<sup>d</sup>, Igor N. Flerov<sup>a,c</sup>

<sup>a</sup> Kirensky Institute of Physics, Federal Research Center KSC SB RAS, 660036, Krasnoyarsk, Russia

<sup>b</sup> Institute of Engineering Systems and Energy, Krasnoyarsk State Agrarian University, 660049, Krasnoyarsk, Russia

<sup>c</sup> Institute of Engineering Physics and Radioelectronics, Siberian Federal University, 660074, Krasnoyarsk, Russia

<sup>d</sup> Institute of Chemistry, Far Eastern Department of RAS, 690022, Vladivostok, Russia

## ARTICLE INFO

### Keywords:

Phase transition  
Fluorides  
Heat capacity  
Entropy  
Thermal expansion  
Birefringence  
Solid solution  
Internal pressure

## ABSTRACT

The effect of a change in internal pressure as a result of partial substitution of the central atom on the realization and stability of the initial and distorted crystalline phases in  $(\text{NH}_4)_3\text{Ti}_x\text{Sn}_{1-x}\text{F}_7$  solid solutions has been studied. It was found that at a Ti concentration in the range of  $x = 0.15\text{--}0.40$ , the reconstructive transition  $Pm\text{-}3m \leftrightarrow Pa\text{-}3$  is transformed into a sequence of phase transitions  $Pm\text{-}3m \leftrightarrow P4/mbm \leftrightarrow P4/mmc \leftrightarrow Pa\text{-}3$ . In the  $(\text{NH}_4)_3\text{Ti}_{0.15}\text{Sn}_{0.85}\text{F}_7$  solid solution, the first-order phase transition between two cubic phases at  $T_0 = 352$  K is characterized by a significant volume jump  $\delta(\Delta V/V_0) \approx 1\%$ , comparable with that in  $(\text{NH}_4)_3\text{SnF}_7$ . An increase of the Ti concentration leads to a strong decrease in the stability of the  $Pm\text{-}3m$  cubic phase: the first tetragonal  $P4/mbm$  phase appears in  $(\text{NH}_4)_3\text{Ti}_{0.4}\text{Sn}_{0.6}\text{F}_7$  at  $T_0 = 400$  K, which proves the existence of the predicted high-temperature cubic phase in  $(\text{NH}_4)_3\text{TiF}_7$ . In solid solutions, a decrease in birefringence and entropy of phase transitions was observed in comparison with the initial compounds with Sn and Ti as central atoms. The role of critical parameters (unit cell volume, temperature, external pressure) in the formation of cubic and distorted phases is discussed.

## 1. Introduction

A lot of chemical compounds of various compositions crystallize in the perovskite cubic structure (sp. gr.  $Pm\text{-}3m$ ,  $Z = 1$ ) and can form a wide variety of low-symmetry distorted structures due to phase transitions associated with temperature or/and pressure changes [1–4]. The field of practical applications of perovskite-like materials, which demonstrate very interesting electric, thermal, optical and other properties, is constantly expanding [5–8]. Depending on the size of the  $A^+$  cation, as well as central atom, the crystal structure of complex heptafluorides with the general chemical formula  $A_3MF_7$ , in other words, double fluoride salts  $A_2MF_6 \bullet AF$ , is also characterized at room temperature by perovskite cubic or distorted structure [8–12]. The seventh fluorine atom does not belong to the  $MF_6$  polyhedron and occupies a special crystallographic position. Recent studies have shown that, above 356 K, the initial  $Pm\text{-}3m$  cubic phase exists in ammonium heptafluorostannate,  $(\text{NH}_4)_3\text{SnF}_7$  (Fig. 1), which is characterized by a significant disorder of structural elements [13]: anionic octahedral  $[\text{SnF}_6]^{2-}$  and cationic

tetrahedral  $[\text{NH}_4]^+$  species occupy several equivalent orientations due to the high symmetry of their crystallographic sites.

Upon cooling,  $(\text{NH}_4)_3\text{SnF}_7$  undergoes a very interesting structural transformation into another low-temperature cubic phase  $Pa\text{-}3$  ( $Z = 8$ ), which is completely ordered. The ordering of octahedra and tetrahedra is also accompanied by the rearrangement of the N–H...F hydrogen bonds, which leads to huge rotations of ordered octahedra (about  $40^\circ$ ) and large displacements of  $F^-$  ions. Since both cubic phases are not related to each other by a group-subgroup relationship, the phase transition between them was characterized as a reconstructive transformation [13].

A change in the internal (chemical) pressure associated with a decrease in the volume of the unit cell as a result of the cationic substitution  $\text{Ti}$  ( $R = 0.605 \text{ \AA}$ )  $\rightarrow$   $\text{Sn}$  ( $R = 0.690 \text{ \AA}$ ), leads to specific features of the formation of the structure in the related heptafluoride  $(\text{NH}_4)_3\text{TiF}_7$  [14]. The cubic  $Pa\text{-}3$  phase was also found in this heptafluoride, but only below room temperature, and upon heating it undergoes successive phase transitions accompanied by the following symmetry changes  $Pa\text{-}3$

\* Corresponding author. Kirensky Institute of Physics, Federal Research Center KSC SB RAS, 660036, Krasnoyarsk, Russia.

E-mail address: [evbogdanov@iph.kasn.ru](mailto:evbogdanov@iph.kasn.ru) (E.V. Bogdanov).

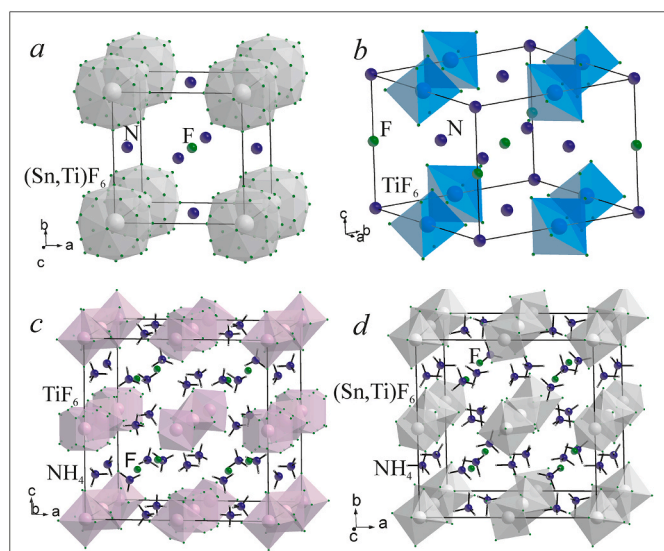


Fig. 1. Crystal structure (a)  $(\text{NH}_4)_3(\text{Sn,Ti})\text{F}_7 - Pm-3m$ , (b)  $(\text{NH}_4)_3\text{TiF}_7 - P4/mbm$ , (c)  $(\text{NH}_4)_3\text{TiF}_7 - P4/mnc$ , (d)  $(\text{NH}_4)_3(\text{Sn,Ti})\text{F}_7 - Pa-3$ .

$(292 \text{ K}) \leftrightarrow P4/mnc (343 \text{ K}) \leftrightarrow P4/mbm$  [15]. The space groups of both tetragonal phases are derivatives of the  $Pm-3m$  group and the transformation between them is ferroelastic in nature. Despite the fact that the  $Pm-3m$  phase is considered the parent phase for  $A_3\text{MF}_7$  compounds, it was not observed in ammonium heptafluorotitanate up to the decomposition temperature of  $\sim 360\text{--}380 \text{ K}$  [15,16]. To clarify this situation, the analysis of the  $T$ - $p$  phase diagram proved to be very fruitful.

Two important points are revealed concerning the possibility of realizing the  $P4/mbm \leftrightarrow Pm-3m$  phase transition in  $(\text{NH}_4)_3\text{TiF}_7$ . First, at atmospheric pressure, it can exist at a temperature of about  $430 \text{ K}$  in the absence of decomposition, second, this transformation can occur at high pressure,  $p > 0.41 \text{ GPa}$ , in the temperature range  $T \leq 300 \text{ K}$  [15]. Thus, the small volume of the unit cell in ammonium heptafluorotitanate compared to  $(\text{NH}_4)_3\text{SnF}_7$  further decreases in the region of the  $Pa-3 \leftrightarrow Pm-3m$  transformation by hydrostatic pressure and low temperature. However, it can be assumed that this moment does not change the ratio between the degrees of ordering/disordering of structural elements in both the high-temperature and low-temperature cubic phases. This assumption was confirmed by the results of calorimetric studies. Within the error of determination, the entropy change associated with the  $Pa-3 \leftrightarrow Pm-3m$  transition turned out to be the same in both heptafluorides:  $\Delta S_0 = 33.5 \pm 3.5 \text{ J/mol}\cdot\text{K}$  in  $(\text{NH}_4)_3\text{SnF}_7$  at atmospheric pressure [17] and  $\sum \Delta S_i = 34.9 \pm 2.5 \text{ J/mol}\cdot\text{K}$  in  $(\text{NH}_4)_3\text{TiF}_7$  at high pressure [15].

Comparison of these data with the results of calculating the corresponding change in entropy within the framework of structural models of both cubic phases ( $\Delta S_0 = 23.1 \text{ J/mol}\cdot\text{K}$ ), which are associated only with reorientational disorder/order of the  $[\text{MF}_6]^{-2}$  octahedra and the  $[\text{NH}_4]^+$  tetrahedra, showed a rather strong discrepancy. One of the reasons is that the contribution of the change in entropy associated with the reconstructive nature of the formation of the  $Pa-3$  phase is not taken into account, which is rather difficult to estimate.

In this work, we study the effect of internal pressure, which changes as a result of partial substitution  $\text{Ti} \rightarrow \text{Sn}$ , on the thermodynamic stability of the initial and distorted phases in solid solutions with the compositions close to pure ammonium heptafluorostannate,  $(\text{NH}_4)_3\text{Ti}_x\text{Sn}_{1-x}\text{F}_7$  ( $x = 0.15, 0.40$ ). Depending on the concentration of titanium, a strong difference was found in the behavior of structural parameters, heat capacity, thermal expansion, optical twinning and birefringence.

## 2. Experimental and results

Colorless transparent single crystals of solid solutions  $(\text{NH}_4)_3\text{Ti}_x\text{Sn}_{1-x}\text{F}_7$  ( $0 < x \leq 0.6$ ) could be obtained on the basis of the cubic modification of  $(\text{NH}_4)_3\text{SnF}_7$  ( $Pa-3$ ,  $Z = 8$ ) [13], while they were not implemented on the basis of the tetragonal modification of  $(\text{NH}_4)_3\text{TiF}_7$  ( $P4/mnc$ ,  $Z = 8$ ) [14]. Two samples with  $x = 0.15$  and  $x = 0.40$  were used for our investigations. The starting materials for their synthesis were crystalline  $(\text{NH}_4)_2\text{SnF}_6$  and  $(\text{NH}_4)_2\text{TiF}_6$ , taken in molar ratio 0.8:0.2 and 0.5:0.5, respectively, which were dissolved in aqueous solution of  $\text{NH}_4\text{F}$  (40 wt %). It should be noted that for the synthesis of heptafluoride complexes from fluoride solutions, the large excess of  $\text{NH}_4\text{F}$  is needed relative to stoichiometry:  $(\text{NH}_4)_2\text{MF}_6 + \text{NH}_4\text{F} = (\text{NH}_4)_3\text{MF}_7$  ( $M = \text{Si, Ge, Sn, Ti, Zr, Hf}$ ). At least, a three- or fourfold excess of  $\text{NH}_4\text{F}$  was taken to obtain polyhedral single crystals of  $(\text{NH}_4)_3\text{Ti}_x\text{Sn}_{1-x}\text{F}_7$  at a solution pH of 6.4–6.7, which was adjusted by  $\text{NH}_3\cdot\text{aq}$ , if necessary. Slow evaporation of the solution in air resulted in several portions of single crystals, which were recovered periodically during the crystallization process, rinsed with ethanol under vacuum and air-dried. The Ti:Sn ratio was monitored by X-ray fluorescence and atomic absorption method. For example, 15 g of the mixture  $[0.5(\text{NH}_4)_2\text{SnF}_6 + 0.5(\text{NH}_4)_2\text{TiF}_6]$  was dissolved in 30 ml of  $\text{NH}_4\text{F}$  (40 wt %) on heating in a water bath, filtered, and evaporated in air in a fume hood. According to atomic absorption, the Ti:Sn ratio in the first portions of the crystals was close to 0.4:0.6. The initial  $[0.8(\text{NH}_4)_2\text{SnF}_6 + 0.2(\text{NH}_4)_2\text{TiF}_6]$  mixture gave a Ti:Sn ratio of 0.15:0.85.

The powder diffraction data of  $(\text{NH}_4)_3\text{Ti}_x\text{Sn}_{1-x}\text{F}_7$  for Rietveld analysis were collected at  $300 \text{ K}$  with a Bruker D8 ADVANCE powder diffractometer (Cu- $K\alpha$  radiation) and linear VANTEC detector. Temperature control was effectively achieved in the experiment by using the Anton Paar TTK-450 equipment, known for its accuracy of  $\pm 0.2 \text{ K}$ . The data was collected in reflection mode (Bragg-Brentano geometry). The step size of  $2\theta$  was  $0.016^\circ$ , and the counting time was 2 s per step. All peaks were indexed by cubic cell ( $Pa-3$ ), with parameters close to the previously studied  $(\text{NH}_4)_3\text{SnF}_7$  [13,14].

Therefore, this structure was taken as starting model for Rietveld refinement which was performed using TOPAS 4.2 [18]. During the refinement process, the positions of hydrogen atoms are adjusted based on the positions of the N atom, allowing the H atoms to be positioned relative to the N atom. To simplify the refinement, a single isotropic thermal parameter is assigned to all hydrogen atoms, reducing the number of refined parameters. The position of central atom in octahedron  $[\text{MF}_6]$  was occupied by  $\text{Ti}^{4+}/\text{Sn}^{4+}$  ions according to suggested chemical formula (Table 1).

Refinements were stable and gave low  $R$ -factors (Fig. 2, Table 2).

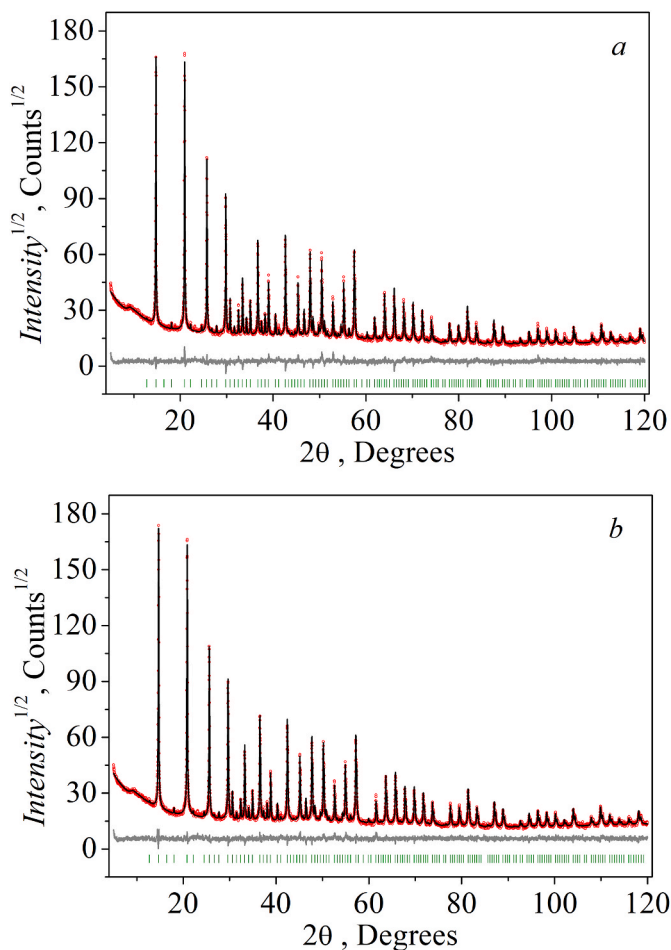
Thus, the results of X-ray studies, firstly, confirmed the realization of solid solutions  $(\text{NH}_4)_3\text{Ti}_x\text{Sn}_{1-x}\text{F}_7$ , and secondly, revealed the same cubic symmetry at room temperature in both synthesized compounds. However, the question of the existence of phase transitions in them remained open. To clarify this situation, variable temperature studies of thermodynamic and optical properties, as well as unit cell parameters, were carried out.

At the first stage, the heat capacity of several powder samples of each solid solution weighing about  $0.2 \text{ g}$  was examined in a wide temperature range of  $100\text{--}400 \text{ K}$  using two differential scanning calorimeters (DSC): DSM-10 M and Netzsch DSC 204 F1 Phoenix. The experiments were carried out in a helium atmosphere in the heating and cooling modes at rates  $dT/dt = \pm (2\text{--}8) \text{ K/min}$ .

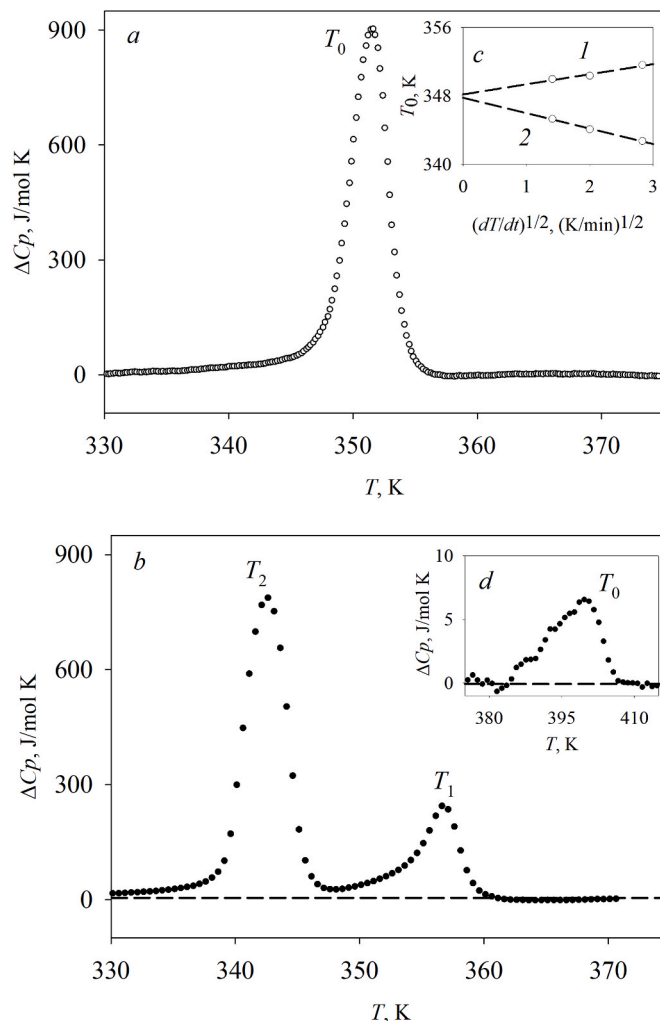
One and three heat capacity anomalies were found for solid solutions with titanium concentrations of 15% and 40%, respectively. Fig. 3 shows the temperature behavior of the excess heat capacity  $\Delta C_p$ , defined as the difference between the total molar heat capacity  $C_p$  and the non-anomalous lattice contribution  $C_{\text{lat}}$ . In the heating mode, the  $\Delta C_p$  peaks were found at  $T_0 = 352 \pm 1 \text{ K}$  for  $x = 0.15$  and  $T_0 = 400 \pm 2 \text{ K}$ ,  $T_1 = 357 \pm 1 \text{ K}$  and  $T_2 = 343 \pm 1 \text{ K}$  for  $x = 0.40$ . Comparison of the obtained results with the data for both initial heptafluorides,  $(\text{NH}_4)_3\text{SnF}_7$  and  $(\text{NH}_4)_3\text{TiF}_7$ , made it possible to assume with certainty that the heat

**Table 1**Fractional atomic coordinates and isotropic displacement parameters ( $\text{\AA}^2$ ) of  $(\text{NH}_4)_3\text{Ti}_x\text{Sn}_{1-x}\text{F}_7$ .

Atom	x	y	z	$B_{\text{iso}}$	Occ.
$x = 0.40$ ( $T = 300$ K)					
Sn1	0	0	0	1.69(17)	0.545(11)
Ti1	0	0	0	1.69(17)	0.455(11)
Sn2	0.5	0	0	2.15(18)	0.632(12)
Ti2	0.5	0	0	2.15(18)	0.368(12)
F1	0.1480(4)	-0.0220(5)	0.0276(6)	4.9(3)	1
F2	0.3886(4)	0.0987(5)	0.0567(3)	2.4(2)	1
F3	0.2616(5)	0.2616(5)	0.2616(5)	4.9(3)	1
N	0.2457(8)	0.2379(6)	0.4853(8)	6.3(3)	1
H1	0.193(11)	0.279(14)	0.519(7)	7.5(3)	1
H2	0.297(7)	0.217(10)	0.536(6)	7.5(3)	1
H3	0.214(15)	0.177(6)	0.455(6)	7.5(3)	1
H4	0.279(11)	0.278(11)	0.432(5)	7.5(3)	1
$x = 0.15$ ( $T = 300$ K)					
Sn1	0	0	0	1.70(16)	0.798(13)
Ti1	0	0	0	1.70(16)	0.202(13)
Sn2	0.5	0	0	1.75(16)	0.841(12)
Ti2	0.5	0	0	1.75(16)	0.159(12)
F1	0.1529(4)	-0.0208(5)	0.0277(6)	5.0(3)	1
F2	0.3901(5)	0.1007(5)	0.0564(3)	2.5(2)	1
F3	0.2609(6)	0.2609(6)	0.2609(6)	5.0(2)	1
N	0.2441(8)	0.2377(6)	0.4901(9)	5.5(2)	1
H1	0.198(8)	0.179(6)	0.497(7)	6.6(3)	1
H2	0.213(8)	0.298(4)	0.521(7)	6.6(3)	1
H3	0.309(4)	0.223(10)	0.525(7)	6.6(3)	1
H4	0.257(8)	0.250(7)	0.4176(19)	6.6(3)	1

**Fig. 2.** Difference Rietveld plot of  $(\text{NH}_4)_3\text{Ti}_x\text{Sn}_{1-x}\text{F}_7$  at  $T = 300$  K: (a)  $x = 0.40$  and (b)  $x = 0.15$ .**Table 2**Main parameters of processing and refinement of  $(\text{NH}_4)_3\text{Ti}_x\text{Sn}_{1-x}\text{F}_7$  solid solutions.

$T$ , K	Space Group	Cell parameters ( $\text{\AA}$ ), Cell Volume ( $\text{\AA}^3$ )	$R_{\text{wp}}$ , $R_p$ , $R_B$ , $\chi^2$
$x = 0.40$			
300	$Pa-3$	$a = 11.99220(15)$ , $V_{\text{cell}} = 1724.63(7)$	7.52, 5.79, 4.39, 1.62
$x = 0.15$			
300	$Pa-3$	$a = 12.05223(17)$ , $V_{\text{cell}} = 1750.66(7)$	6.80, 5.28, 2.03, 1.48

**Fig. 3.** Excess heat capacity of  $(\text{NH}_4)_3\text{Ti}_x\text{Sn}_{1-x}\text{F}_7$ : (a)  $x = 0.15$  and (b, d)  $x = 0.40$  at  $dT/dr = 8$  K/min. (c) Dependence of the phase transition temperature of  $(\text{NH}_4)_3\text{Ti}_{0.15}\text{Sn}_{0.85}\text{F}_7$  on the value of  $dT/dt$  upon heating (1) and cooling (2).

capacity anomalies found in solid solutions are associated with phase transitions.

At a temperature cycling rate of 8 K/min, the phase transformation in the sample with  $x = 0.15$  is accompanied by a sufficiently large temperature hysteresis  $\delta T_0 = 9$  K. To determine the actual hysteresis corresponding to quasi-equilibrium conditions, we analyzed the dependence of the temperature  $T_0$  on the heating/cooling rate (Fig. 3c). Extrapolation of the experimental dependence  $T_0(dT/dr)^{1/2}$  to  $dT/dr = 0$  leads to the following parameters:  $T_0 = 348$  K and  $\delta T_1 \approx 0.5$  K. The temperature hysteresis defined by this way showed that the phase

transition in  $(\text{NH}_4)_3\text{Ti}_{0.15}\text{Sn}_{0.85}\text{F}_7$  is a first order transformation quite close to the tricritical point, similarly to  $(\text{NH}_4)_3\text{SnF}_7$  [17].

Linear thermal expansion measurements were performed using a pushrod dilatometer NETZSCH model DIL-402C with a fused silica sample holder. The experiments were carried out in a dry helium flow in the temperature range 100–300 K at a heating rate of 3 K/min.

Two types of samples were examined: small single crystals ~ 1–2 mm in size and quasi-ceramic tablets 8 mm in diameter, 2–4 mm high and weighing ~ 0.04–0.06 g prepared by pressing powdered  $(\text{NH}_4)_3\text{Ti}_x\text{Sn}_{1-x}\text{F}_7$  at  $p \leq 2$  GPa. Heat treatment was not carried out due to the presence of ammonium ions, since prolonged exposure of the sample at  $T > (350\text{--}400)$  K led to partial decomposition of the starting compound and the formation of  $(\text{NH}_4)_2\text{SnF}_6$  as an impurity [17]. Analysis of the microstructure parameters and images of the ceramic surface topography was performed using a SU3500 scanning electron microscope (SEM) (Fig. 4).

Both quasi-ceramic samples are rather dense and display compact microstructures with an average grain size of about 1.3–1.5  $\mu\text{m}$ . X-ray studies did not show the formation of texture, i.e., the preferred orientation of small crystallites, when subjected to pressure during the production of ceramic samples.

Fig. 5 shows the temperature dependences of the volumetric strain  $\Delta V/V_0 = 3(\Delta L/L_0)$  and the volumetric thermal expansion coefficient  $\beta = 3\alpha$  ( $\alpha$  is the linear thermal expansion coefficient). Strain in the ceramics with  $x = 0.15$  demonstrates an anomalous increase well below the temperature  $T_0 \approx 351$  K, at which a significant jump in volume is

observed,  $\delta V/V_0 \approx 0.8\%$  (Fig. 5a).

At temperatures close to  $T_b$  found by measuring the heat capacity, the ceramic  $(\text{NH}_4)_3\text{Ti}_{0.4}\text{Sn}_{0.6}\text{F}_7$  sample showed, three rather small anomalies in the  $\Delta V/V_0(T)$  dependence, which are more pronounced in the behavior of  $\beta(T)$ . Only the change in strain at  $T_2 = 343$  K looks like it is associated with a first order transformation.

Measurements performed on unoriented single-crystal samples revealed a thermal expansion behavior similar to that observed for both ceramic samples (Fig. 5). However, all anomalies became more pronounced as evidenced by the increase in volume jumps at  $T_0$  ( $\delta V_0/V_0 \approx 0.8\% \rightarrow 1.0\%$ ) in  $(\text{NH}_4)_3\text{Ti}_{0.15}\text{Sn}_{0.85}\text{F}_7$  and at  $T_2$  ( $\delta V_2/V_0 \approx 0.2\% \rightarrow 0.5\%$ ) in  $(\text{NH}_4)_3\text{Ti}_{0.4}\text{Sn}_{0.6}\text{F}_7$ . Both single crystals also demonstrate a relatively small increase in the temperatures of all phase transitions by ~ (1.5–3.0 K) as compared to ceramics.

The increase in the volume jump in the single-crystal sample of  $(\text{NH}_4)_3\text{Ti}_x\text{Sn}_{1-x}\text{F}_7$   $x = 0.15$  can be due to the presence of growth stresses, which are removed during the reconstructive phase transition by cracking of the sample.

The results of studying the temperature dependences of deformation using dilatometer quite satisfactory correspond to the data on the behavior of the unit cell parameters obtained by XRD (Fig. 6, Supplementary). In both cases, the relative changes in volume during phase transitions of the first order in both solid solutions are close: about  $\delta V/V_0 \approx 1\%$  ( $Pm\text{-}3m \leftrightarrow Pa\text{-}3$ ,  $x = 0.15$ ) and  $\delta V/V_1 \approx \sim 0.1\%$  ( $P4/mnc \leftrightarrow Pa\text{-}3$ ,  $x = 0.40$ ).

A relatively small jump in volumetric deformation in  $(\text{NH}_4)_3\text{Ti}_{0.4}\text{Sn}_{0.6}\text{F}_7$  as a result of the reconstructive transformation at  $T_2$  is a consequence of the opposite sign of rather large changes in linear deformations  $\delta(\Delta L/L_1)$  along the axes  $a_{\text{tet}}$  and  $c_{\text{tet}}$ : +0.6% and –1.2%, respectively (Fig. 6a). Unfortunately, the features of the X-ray setup did not allow measurements of the unit cell parameters above 370 K and again, as in the case of  $(\text{NH}_4)_3\text{TiF}_7$  [14], we could not obtain information about the cell parameter in the  $Pm\text{-}3m$  phase.

The examination of the stability of crystalline phases in  $(\text{NH}_4)_3\text{Ti}_x\text{Sn}_{1-x}\text{F}_7$  solid solutions was also performed by optical studies using an Axioskop-40 polarizing microscope and a Linkam LTS 350 temperature chamber in the temperature range of 90–450 K. The studies were carried out on selected growth crystal plates (with a thickness of about 500  $\mu\text{m}$ ) with a (001)<sub>c</sub> orientation determined by X-ray diffraction. To prevent decomposition when heated, the samples were placed in oil under the cover glass. Birefringence was measured by a Berek compensator (“Leica”) with an accuracy of  $\pm 10^{-5}$ .

The optical study in polarized light showed that, upon heating in a wide temperature range, the  $(\text{NH}_4)_3\text{Ti}_{0.15}\text{Sn}_{0.85}\text{F}_7$  crystal remains optically isotropic, i.e. cubic. However, the change in symmetry associated with the transition between two cubic phases was detected at temperatures  $T_{01} = 358$  K and  $T_{01} = 352$  K during heating and cooling, respectively, as the appearance of light spots and the movement of the front formed by them in the optical picture during a phase transition. This phenomenon can be due to the mechanical stresses that arise at the boundaries of the sharp difference in the volumes of the unit cells of the two cubic phases. As a result, small cracks appeared in the sample and disappeared, that is, “healed”, immediately after the formation of the homogeneous phase in the entire sample, that is, after transformation. This pattern was observed during repeated multiple thermal cycling. Macroscopic cracking of the samples as a result of these procedures was also not observed (Fig. 7).

The  $(\text{NH}_4)_3\text{Ti}_{0.4}\text{Sn}_{0.6}\text{F}_7$  sample undergoes a sequence of three optical transformations upon heating from room temperature. At  $T < 337$  K, the cubic symmetry of the low-temperature phase is characterized by the absence of optical anisotropy in the sample. The appearance and disappearance of a twin structure occurs as a result of a decrease in the symmetry of the crystal during the phase transition at temperatures  $T_{21} = 344$  K and  $T_{21} = 337$  K during thermal cycling (Fig. 8 a, b). The character of twin extinction in polarized light indicates the tetragonal symmetry of the distorted phase. Near the temperature  $T_1 \approx 358$  K, the twinning

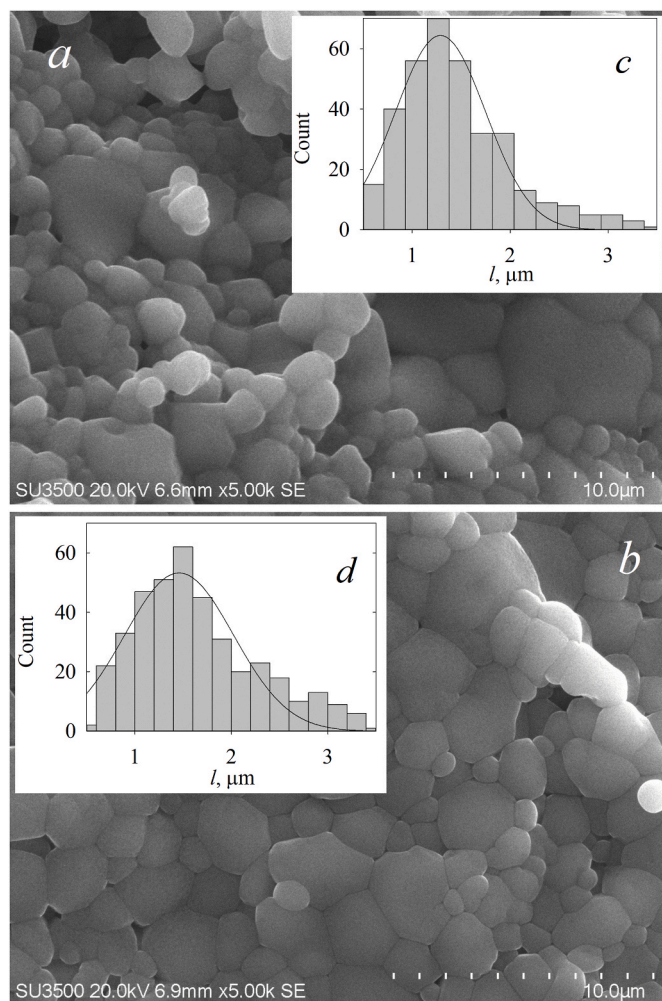


Fig. 4. SEM images (a, b) of fresh scrap and (c, d) average grain sizes of quasi-ceramics  $(\text{NH}_4)_3\text{Ti}_x\text{Sn}_{1-x}\text{F}_7$  with  $x = 0.15$  and  $0.40$ , respectively.

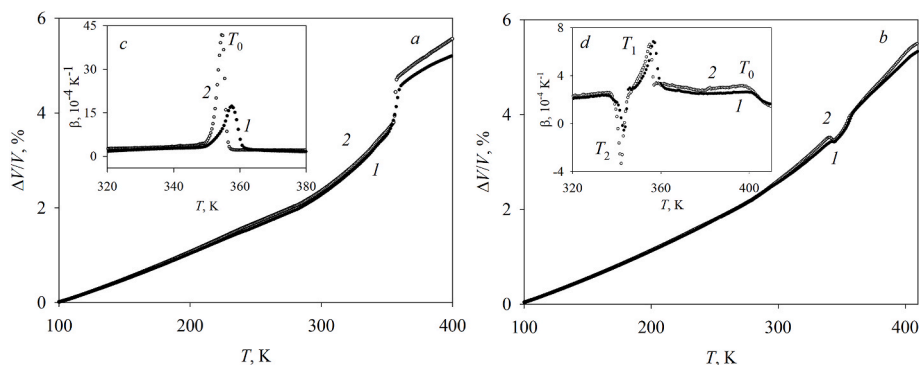


Fig. 5. Temperature dependences (a, b) of volumetric deformation and (c, d) coefficient of volumetric thermal expansion of (1) ceramic and (2) crystalline solid solutions  $(\text{NH}_4)_3\text{Ti}_x\text{Sn}_{1-x}\text{F}_7$ . (a, c)  $x = 0.15$  and (b, d)  $x = 0.40$ .

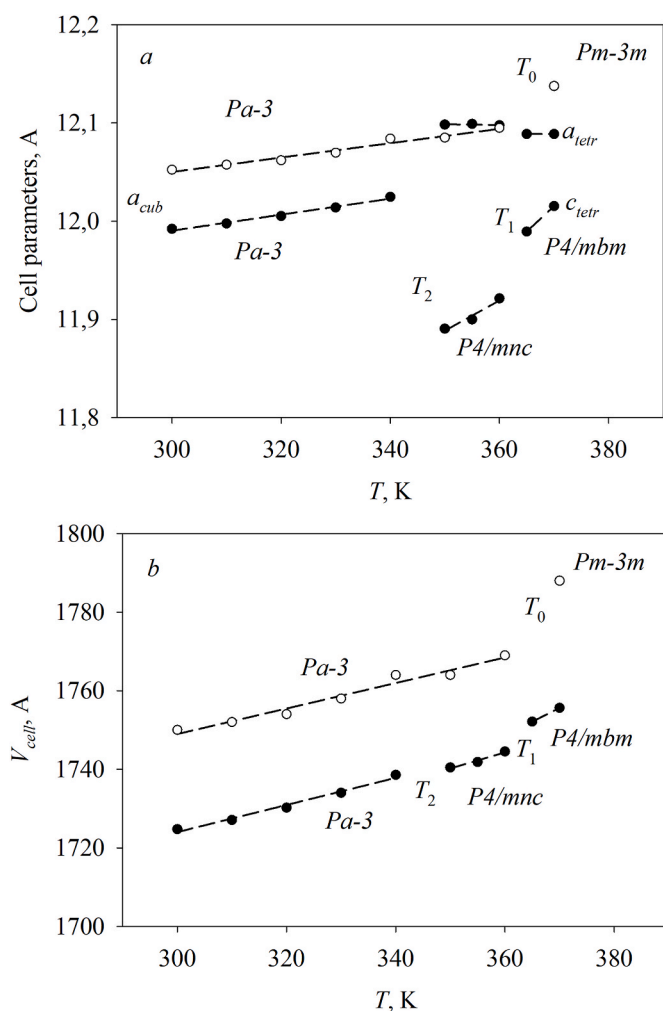


Fig. 6. Temperature dependences of (a) cell parameters and (b) cell volumes of  $(\text{NH}_4)_3\text{Ti}_x\text{Sn}_{1-x}\text{F}_7$ . Open and close dot – experimental results of XRD for sample with  $x = 0.15$  and  $x = 0.40$ , respectively.

pattern becomes more complicated and a transition to another tetragonal phase is observed (Fig. 8c). Above  $T_0 = 400$  K,  $(\text{NH}_4)_3\text{Ti}_{0.4}\text{Sn}_{0.6}\text{F}_7$  again becomes optically isotropic, i.e. undergoes a phase transition to a high-temperature cubic phase. Thus, since the sequence of the syngony changes in this solid solution is similar to that observed for  $(\text{NH}_4)_3\text{TiF}_7$  [13,16], there is no reason to doubt that both compounds undergo the same sequence of phase transitions.

The temperature dependence of birefringence was measured on a

single-domain sample of the (100)-cut (Fig. 9). Upon heating, optically isotropic at room temperature  $(\text{NH}_4)_3\text{Ti}_{0.4}\text{Sn}_{0.6}\text{F}_7$  undergoes a transition at  $T_2 = 344$  K to a low-temperature tetragonal phase accompanied by the appearance of a birefringence. Near  $T_1 \approx 358$  K, the rearrangement of the twin structure is observed, which is associated with the transition to the high-temperature tetragonal phase.

As the temperature increases from  $T_2$ , the optical anisotropy gradually decreases and becomes equal to zero at  $T_0 = 400$  K, where the high-temperature cubic phase occurs. On the whole, the behavior of birefringence in the sample with  $x = 0.40$  is similar to that in  $(\text{NH}_4)_3\text{TiF}_7$  [16] (Fig. 9), in which the parent  $Pm-3m$  cubic phase was not achieved due to the rather low temperature of crystal decomposition at atmospheric pressure. However,  $(\text{NH}_4)_3\text{Ti}_{0.4}\text{Sn}_{0.6}\text{F}_7$  is characterized by a rather small birefringence, even the maximum value of  $\Delta n = n_o - n_e = 0.00096$ , is only  $\sim 44\%$  of the value of  $\Delta n$  at  $T_3$  in  $(\text{NH}_4)_3\text{TiF}_7$  (Fig. 9).

In addition, it can be seen that the change in the chemical pressure associated with the partial replacement of the Ti cation by the mixed Ti/Sn ion plays an important role in the formation of the stability of the crystalline phases, as well as the optical properties. Indeed, firstly, a strong increase in temperature  $T_2$  is observed in the solid solution, while the transformation between two tetragonal phases is shifted to a lesser extent and has features of a second-order transformation.

### 3. Discussion

Since the behavior of thermal properties, unit cell parameters, birefringence, optical twinning, as well as the character of the alternation of syngonies of crystalline phases in solid solutions  $(\text{NH}_4)_3\text{Ti}_x\text{Sn}_{1-x}\text{F}_7$  with  $x = 0.15$  and  $0.40$  are similar to those observed, respectively, in  $(\text{NH}_4)_3\text{SnF}_7$  and  $(\text{NH}_4)_3\text{TiF}_7$  [13,14], it can be safely assumed that, when heated, the solid solutions under study undergo the corresponding sequences of structural transformations:  $Pa-3 \leftrightarrow Pm-3m$  and  $Pa-3 \leftrightarrow P4/mnc \leftrightarrow P4/mbm \leftrightarrow Pm-3m$ .

The existence of the  $Pm-3m$  cubic phase as the initial high-temperature phase in both studied samples, as well as in  $(\text{NH}_4)_3\text{SnF}_7$ , confirmed two earlier assumptions: firstly, that this phase is the parent phase for  $A_3MF_7$  heptafluorides [14] and, secondly, that it is not observed in  $(\text{NH}_4)_3\text{TiF}_7$  because of its low decomposition temperature [17].

The thermodynamic stability of all crystalline phases in  $(\text{NH}_4)_3\text{Ti}_x\text{Sn}_{1-x}\text{F}_7$  strongly depends on the concentration ratio of  $\text{Ti}^{4+}$  and  $\text{Sn}^{4+}$  ions or, in other words, on the effective ionic radius of the central atom. Upon cooling,  $(\text{NH}_4)_3\text{Ti}_{0.15}\text{Sn}_{0.85}\text{F}_7$  ( $R_{\text{Ti}/\text{Sn}} = 0.678$  Å) undergoes a transformation between two cubic phases at a temperature  $T_0 = 352$  K, which is close to  $T_0$  observed in  $(\text{NH}_4)_3\text{SnF}_7$  ( $R_{\text{Sn}} = 0.690$  Å) [17], whereas in  $(\text{NH}_4)_3\text{TiF}_7$  ( $R_{\text{Ti}} = 0.605$  Å) the  $Pm-3m \leftrightarrow Pa-3$  transition was found only at high pressure,  $p > 0.4$  GPa, below 298 K [15]. In the sample with  $x = 0.15$ , this phase transition remains a first order

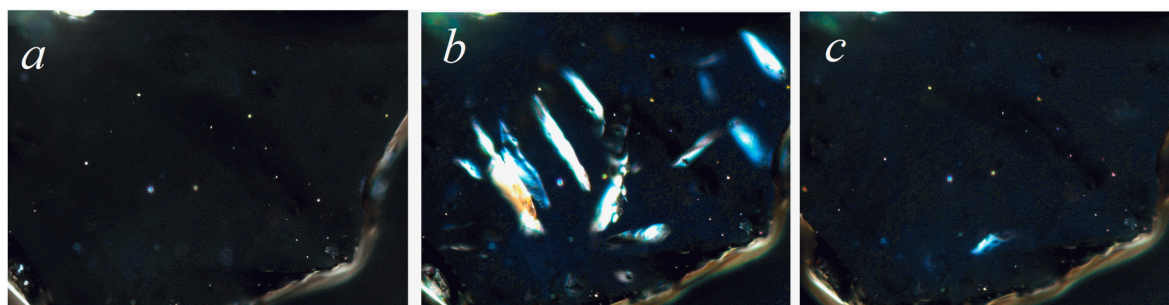


Fig. 7. Observation of the phase front movement in the crystal plate of  $(\text{NH}_4)_3\text{Ti}_{0.15}\text{Sn}_{0.85}\text{F}_7$  during cooling from high-temperature cubic phase to low-temperature one: (a) 353 K, (b)  $T_0 = 352$  K, (c) 351 K.

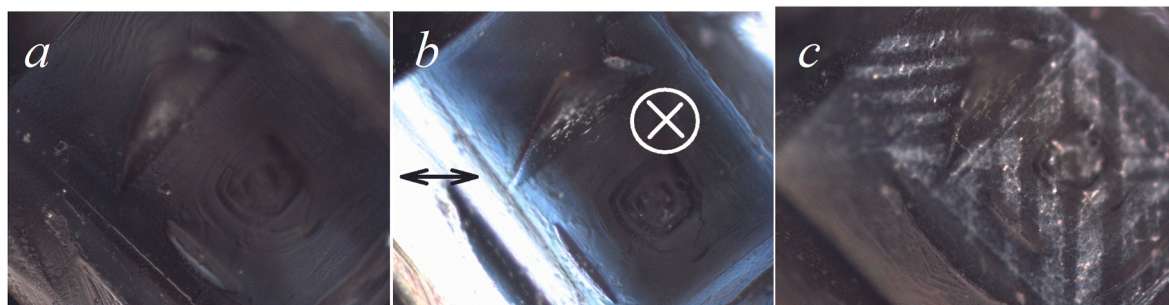


Fig. 8. Twin pattern in distorted phases of  $(\text{NH}_4)_3\text{Ti}_{0.4}\text{Sn}_{0.6}\text{F}_7$  observed along the  $[001]_c$  axis.  $T = 350$  K (low-temperature tetragonal phase): (a) a twin with a horizontal axis of the fourth order becomes clear, (a, b) a twin with a vertical exit of the optical axis always remains dark. (c) Visualization of new twins near  $T = 380$  K (high-temperature tetragonal phase).

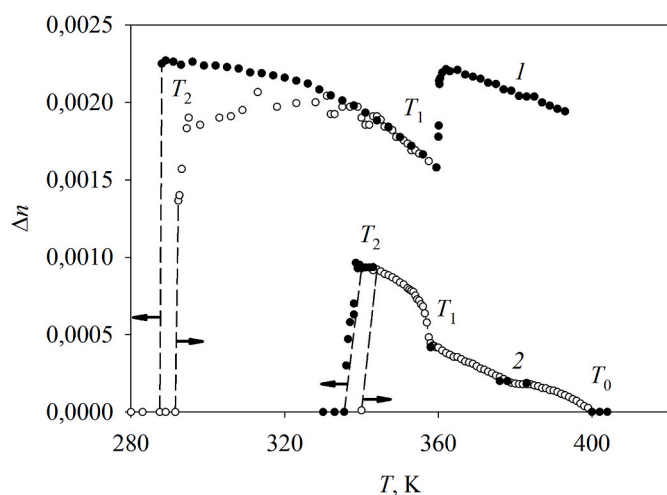


Fig. 9. Temperature dependences of the main birefringence of (1)  $(\text{NH}_4)_3\text{TiF}_7$  crystal [15] and (2)  $(\text{NH}_4)_3\text{Ti}_{0.4}\text{Sn}_{0.6}\text{F}_7$  solid solution in heating (open symbols) and cooling (closed symbols) modes.

transformation and is accompanied by a relatively small temperature hysteresis,  $\delta T_1 \approx 0.5$  K, which indicates its proximity to the tricritical point, as is typical for  $(\text{NH}_4)_3\text{SnF}_7$  ( $\delta T_1 \leq 1.0$  K) [13,17].

A further decrease in the size of the central atom is accompanied by the appearance of two intermediate tetragonal phases in  $(\text{NH}_4)_3\text{Ti}_{0.4}\text{Sn}_{0.6}\text{F}_7$  ( $R_{\text{Ti/Sn}} = 0.656 \text{ \AA}$ ) with a rather narrow temperature range of their overall stability ( $T_0 - T_2 \approx 60$  K) compared to  $(\text{NH}_4)_3\text{TiF}_7$  ( $T_0 - T_2 \approx 140$  K). It is necessary to point out two very interesting experimental points related to the transformation between two tetragonal phases. First, at sample with  $x = 0.40$  this phase transition at  $T_1 = 357$  K, which is very close to  $T_1 = 358$  K in  $(\text{NH}_4)_3\text{TiF}_7$  [15] and temperature of the direct phase transition  $Pm-3m \leftrightarrow Pa-3$  in

$(\text{NH}_4)_3\text{Ti}_{0.15}\text{Sn}_{0.85}\text{F}_7$  (see above) as well as in  $(\text{NH}_4)_3\text{SnF}_7$  [17]. Second, the behavior of the thermal and optical properties exhibits features of a second-order transformation, which are revealed as a smooth increase in  $\Delta C_p$  upon heating from  $T_2$  to  $T_1$  (Fig. 3), coinciding with a gradual decrease in birefringence in the same temperature range (Fig. 9). Whereas, in ammonium heptafluorotitanate, the  $P4/mbm \leftrightarrow P4/mnc$  phase transition is a first-order transition accompanied by jumps in  $\Delta S$  and  $\Delta n$  at  $T_1$  [16,17].

The data of calorimetric measurements using DSC were analyzed to obtain information about the entropies,  $\Delta S_i$ , associated with phase transitions in both solid solutions. For this aim, the area under the  $\Delta C_p/T$

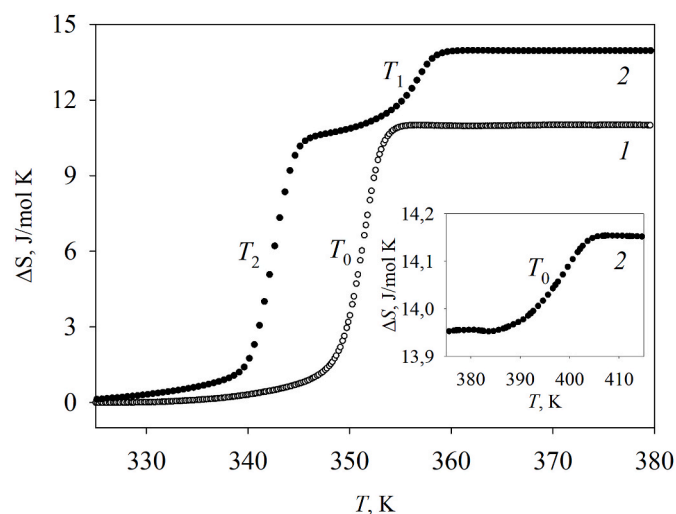


Fig. 10. Temperature dependences of the entropy of phase transitions in  $(\text{NH}_4)_3\text{Ti}_x\text{Sn}_{1-x}\text{F}_7$  solid solutions with  $x = 0.15$  (1) and  $x = 0.40$  (2). The insert shows the change in entropy at  $T_0$  in  $(\text{NH}_4)_3\text{Ti}_{0.4}\text{Sn}_{0.6}\text{F}_7$ .

( $T$ ) curves was integrated. Fig. 10 shows a rather narrow temperature range for the existence of anomalous entropies.

One of the possible reasons for this phenomenon is related to the insufficient high sensitivity of the DSC method to obtain information on pretransition effects during structural rearrangement, which initiate the presence of excess heat capacity/entropy in a wide temperature range below the phase transition point, as was observed on the dependences  $\Delta C_p(T)$  and  $\Delta S(T)$  for  $(\text{NH}_4)_3\text{SnF}_7$  and  $(\text{NH}_4)_3\text{TiF}_7$  studied with a high sensitivity adiabatic calorimeter [15,17].

As a result, the change in entropy during the  $Pa-3 \leftrightarrow Pm-3m$  phase transition in  $(\text{NH}_4)_3\text{Ti}_{0.15}\text{Sn}_{0.85}\text{F}_7$ ,  $\Delta S_0 = 10.9 \pm 1.2$  J/mol·K, is much smaller in comparison with the total entropy change in  $(\text{NH}_4)_3\text{SnF}_7$  ( $\Delta S_0 = 33.5 \pm 3.5$  J/mol·K) undergoing the same structural transformation. Nevertheless,  $\Delta S_0 \sim R \cdot \ln 4$  in solid solution remains characteristic of the order-disorder transformation.

A similar situation is observed in the entropy changes during the sequence of phase transitions in  $(\text{NH}_4)_3\text{Ti}_x\text{Sn}_{1-x}\text{F}_7$  at  $x = 0.40$ :  $\Delta S_0 = 0.2 \pm 0.1$  J/mol·K,  $\Delta S_1 = 3.3 \pm 0.5$  J/mol·K and  $\Delta S_2 = 10.1 \pm 1.1$  J/mol·K, which are much less compared to  $(\text{NH}_4)_3\text{TiF}_7$  [15]. Here, it is also appropriate to pay attention to the strong difference in the values of birefringence in these two compounds (Fig. 9).

On the one hand, since both tetragonal phases are ferroelastic in nature, birefringence may reflect the behavior of the phase transition order parameter,  $\eta$ . If so, then the decrease in  $\eta$  in a solid solution will be accompanied by a decrease in entropy change, since, in accordance with the thermodynamic theory of phase transitions,  $\Delta S_i \sim \eta_i^2$  [19]. On the other hand, it is possible that the reason for the decrease in both values,  $\Delta S$  and  $\Delta n$ , may be due to the fact that the  $P4/mbm - P4/mnc$  phase transition occurs only in those parts of the crystal lattice that are occupied by atoms Ti. Then the entropy and birefringence should increase with increasing titanium concentration. To clarify this ambiguous situation, it is undoubtedly necessary to perform detailed studies of the heat capacity of both  $(\text{NH}_4)_3\text{Ti}_x\text{Sn}_{1-x}\text{F}_7$  compounds ( $x = 0.15$  and  $0.40$ ), but also of other solid solutions using an adiabatic calorimeter, which we plan to carry out in the near future.

As shown in Fig. 6,  $(\text{NH}_4)_3\text{Ti}_{0.4}\text{Sn}_{0.6}\text{F}_7$  demonstrates a strong anisotropic behavior of the unit cell parameters at  $T_2$ . The opposite signs of the changes in the parameters  $a_{tet} - a_{cub}$  and  $c_{tet} - a_{cub}$  show that uniaxial mechanical stresses along different axes can initiate a conventional or inverse piezocaloric effect (PCE), which is a change in entropy/temperature at uniaxial pressure under isothermal/adiabatic conditions. Thus, the results of high-precision calorimetric experiments will also be used to reveal the piezocaloric efficiency of heptafluorides by means of the analysis of the entropy-temperature-uniaxial stress diagram.

Summarizing the results obtained, we can assume that there are some "critical" parameters that characterize the stability of crystalline phases in the series of ammonium heptafluorides  $(\text{NH}_4)_3\text{Ti}_x\text{Sn}_{1-x}\text{F}_7$  ( $x = 0-1$ ). For their detailed quantitative evaluation, it is necessary to continue thorough studies of the structure and physical properties of solid solutions with a different size of the Ti/Sn mixed central atom. Nevertheless, here we will try to give at least their qualitative characteristics.

The first parameter is the unit cell volume,  $V_{cell}$ , the change of which, associated with the substitution of the central atom, leads to a change in the chemical pressure. The data available today allow us to consider that the critical magnitude of  $V_{cell}$  lies between the values typical for the samples with  $x = 0.15$  and  $x = 0.40$  (Table 1). Indeed, in this range of titanium concentrations, the  $Pm-3m \leftrightarrow Pa-3$  phase transition line splits into phase boundaries corresponding to the sequence of structural transformations  $Pm-3m \leftrightarrow P4/mbm \leftrightarrow P4/mnc \leftrightarrow Pa-3$ . The following question also remains open: which of the two tetragonal phases is realized first as  $V_{cell}$  decreases?

Temperature is the second critical parameter that determines the splitting of phase boundaries mentioned above. It is possible that for the system of solid solutions under consideration this temperature lies in the region of 350–360 K. This is indicated by the closeness of the values of  $T_1$

for compositions with  $x = 1$ ; 0.40 and  $T_0$  ( $x = 0.15$ ; 0).

The third, no less important parameter is the external hydrostatic pressure. We can consider that for  $(\text{NH}_4)_3\text{TiF}_7$  its critical value corresponds to the pressure of the second triple point,  $\sim 0.4$  GPa, on the  $T$ - $p$  phase diagram, where three phases  $Pm-3m$ ,  $P4/mnc$  and  $Pa-3$  coexist [16]. Above this pressure, a direct phase transition  $Pm-3m \leftrightarrow Pa-3$  occurs.

Thus, a decrease in the unit cell volume due to a decrease in the size of the Ti/Sn mixed central atom and under the action of hydrostatic pressure leads to opposite effects. In the former case, intermediate phases appear due to splitting of the line of equilibrium phase transition  $Pm-3m \leftrightarrow Pa-3$  and in the latter case, wedding out of these phases is observed,

This contradiction is not so surprising, since a decrease in  $V_{cell}$  during cation-anion substitution can lead not to an increase, but to a decrease in chemical pressure due to an increase in the distances between the critical atoms, i.e., responsible for structural distortions, the interaction of which determines the chemical pressure. The situation observed for ammonium heptafluorides is not unique. A similar phenomenon was observed, for example, for a number of  $\text{Rb}_2\text{KMF}_6$  ( $M$ : Sc, In, Lu, etc.) elpasolites, also formed by substitution of the central atom [20].

#### 4. Conclusions

Analysis of the experimental results on the heat capacity, thermal expansion, unit cell parameters, birefringence, optical twinning, and the character of the alternation of syngonies of crystalline phases showed that it can be confidently stated that, when heated, solid solutions  $(\text{NH}_4)_3\text{Ti}_x\text{Sn}_{1-x}\text{F}_7$  undergo the following sequences of phase transitions:  $x = 0.15 - Pa-3 \leftrightarrow Pm-3m$ ;  $x = 0.40 - Pa-3 \leftrightarrow P4/mnc \leftrightarrow P4/mbm \leftrightarrow Pm-3m$ . Thus, the  $Pm-3m$  cubic phase is indeed the parent phase of complex  $A_3\text{MF}_7$  heptafluorides.

Despite different sequences of phase transitions, the main contribution to the deformation of the crystal lattice of the investigated compounds  $(\text{NH}_4)_3\text{Ti}_x\text{Sn}_{1-x}\text{F}_7$  is associated with the rearrangement of the structure during the formation of the low-temperature  $Pa-3$  phase, which is confirmed by an anomalously large change in entropy.

A strong decrease in the size of the central atom in  $(\text{NH}_4)_3\text{Ti}_{0.15}\text{Sn}_{0.85}\text{F}_7$  ( $R_{\text{Ti/Sn}} = 0.678$  Å) compared to  $(\text{NH}_4)_3\text{SnF}_7$  ( $R_{\text{Sn}} = 0.690$  Å) did not affect the stability temperature of the  $Pm-3m$  phase.

An increase in the Ti concentration to 40 % is accompanied by the appearance of successive transformations  $Pm-3m \rightarrow P4/mbm \rightarrow P4/mnc \rightarrow Pa-3$ , similar to those found in  $(\text{NH}_4)_3\text{TiF}_7$ . The temperature of the  $Pm-3m$  phase stability is 44 K higher than in  $(\text{NH}_4)_3\text{SnF}_7$  and, thus, our assumption that the  $Pa-3 \leftrightarrow Pm-3m$  transition temperature in  $(\text{NH}_4)_3\text{TiF}_7$  exists, but lies above the decomposition temperature [15,16] is correct.

The appearance of the intermediate tetragonal phase  $P4/mbm$  in  $(\text{NH}_4)_3\text{Ti}_{0.4}\text{Sn}_{0.6}\text{F}_7$  occurs at a temperature  $T_1$  very close to the temperature of the phase transition  $Pa-3 \rightarrow Pm-3m$ ,  $T_0$ , in heptafluorostannate and solid solution with  $x = 0.15$ .

To reveal the reason for the decrease in the entropy of phase transitions and birefringence in  $(\text{NH}_4)_3\text{Ti}_x\text{Sn}_{1-x}\text{F}_7$  ( $x = 0.15$ ; 0.40) in comparison with the initial ammonium heptafluorides, detailed studies, including the method of adiabatic calorimeter, of a larger number of solid solutions are required.

To characterize the stability of crystalline phases in ammonium heptafluorides, it is proposed to consider three critical parameters: unit cell volume, temperature, and external pressure.

#### CRedit authorship contribution statement

**Evgeniy V. Bogdanov:** Investigation, Data curation, Visualization, Formal analysis, Writing – original draft, Funding acquisition. **Evgeniy I. Pogoreltsev:** Investigation, Data curation, Formal analysis. **Mikhail V. Gorev:** Investigation, Formal analysis, Writing – review & editing. **Svetlana V. Mel'nikova:** Investigation, Data curation, Formal analysis.

**Maxim S. Molokeyev:** Investigation, Data curation, Formal analysis.  
**Natalia M. Laptash:** Resources, Data curation, Formal analysis. **Igor N. Flerov:** Conceptualization, Methodology, Supervision, Writing – review & editing.

#### Declaration of competing interest

The authors declare that they have no known competing financial interests or personal relationships that could have appeared to influence the work reported in this paper.

#### Data availability

Data will be made available on request.

#### Acknowledgements

The study was supported by a grant from the Russian Science Foundation № 23-22-00115, <https://rscf.ru/project/23-22-00115/>

X-ray and dilatometric data and SEM images were obtained using the equipment of the Krasnoyarsk Regional Center for Collective Use of the Federal Research Center — Krasnoyarsk Science Center of the Siberian Branch of the Russian Academy of Sciences. We are grateful to Dr. A.V. Shabanov for examination of the SEM images.

#### Appendix A. Supplementary data

Supplementary data to this article can be found online at <https://doi.org/10.1016/j.jssc.2023.124373>.

#### References

- [1] K.S. Aleksandrov, A.T. Anistratov, B.V. Beznosikov, N.V. Fedoseeva, Phase Transitions in Crystal Halides  $ABX_3$ , Nauka, Novosibirsk, 1981.
- [2] K.S. Aleksandrov, B.V. Beznosikov, Perovskite-like Crystals, Nauka, Novosibirsk, 1997.
- [3] K. Aleksandrov, S. Beznosikov, B.V. Perovskites, Present and Future. Variety of Parent Phases, Phase Transitions, Possibilities of Synthesis of New Compounds, Nauka, Novosibirsk, 2004.
- [4] R.H. Mitchel, Perovskites, Modern and Ancient, Almaz Press, Inc. Ontario, Canada, 2002, p. 318.
- [5] B.R. Sutherland, E.H. Sargent, Perovskite photonic sources, Nat. Photonics 10 (2016) 295–302, <https://doi.org/10.1038/nphoton.2016.62>.
- [6] Y. Fu, H. Zhu, J. Chen, M.P. Hautzinger, X.-Y. Zhu, S. Jin, Metal halide perovskite nanostructures for optoelectronic applications and the study of physical properties, Nat. Rev. Mater. 4 (2019) 169–188, <https://doi.org/10.1038/s41578-019-0080-9>.
- [7] A. Celeste, F. Capitani, Hybrid perovskites under pressure: present and future directions, J. Appl. Phys. 132 (2022), 220903, <https://doi.org/10.1063/5.0128271>.
- [8] Christian Plitzko, Gerd Meyer, Kristallstruktur von  $(NH_4)_3SnF_7$ : ein Doppelsalz gemäß  $(NH_4)_3[SnF_6]F$  und kein  $(NH_4)_4SnF_8$ , Z. Anorg. Allg. Chem. 623 (1997) 1347–1348, <https://doi.org/10.1002/zaac.19976230903>.
- [9] Chr Plitzko, G. Meyer, Crystal structure of triammonium heptafluorogermanate,  $(NH_4)_3GeF_7$ , Z. Kristallogr. - New Cryst. Struct. 213 (1998), <https://doi.org/10.1524/ncrs.1998.213.14.503>, 503–503.
- [10] U. Reusch, E. Schweda, In situ X-ray powder diffraction: the reactions of Pb (IV)-fluoride with ammonia and  $NH_4F$ , Mater. Sci. Forum 378 (2001), <https://doi.org/10.4028/www.scientific.net/MSF.378-381.326>. Trans Tech Publications Ltd.
- [11] J.L. Hoard, M.B. Williams, Structures of complex fluorides. Ammonium hexafluosilicate - ammonium fluoride,  $(NH_4)_2SiF_6 \cdot NH_4F$ , J. Am. Chem. Soc. 64 (1942) 633–637.
- [12] B. Hofmann, R. Hoppe, Zur Kenntnis des  $(NH_4)_3SiF_7$ -Typs. Neue Metallfluoride  $A_3MF_7$  mit  $M = Si, Ti, Cr, Mn, Ni$  und  $A = Rb, Cs$  Z. Anorg. Allg. Chem. 458 (1979) 151–162.
- [13] I.N. Flerov, M.S. Molokeyev, N.M. Laptash, A.A. Udovenko, E.I. Pogoreltsev, S. V. Mel'nikova, S.V. Misyul, Structural transformation between two cubic phases of  $(NH_4)_3SnF_7$ , J. Fluor. Chem. 178 (2015) 86–92, <https://doi.org/10.1016/j.jfluchem.2015.06.024>.
- [14] M.S. Molokeyev, S.V. Misyul, I.N. Flerov, N.M. Laptash, Reconstructive phase transition in  $(NH_4)_3TiF_7$  accompanied by the ordering of  $TiF_6$  octahedra, Acta Crystallogr. B70 (2014) 924–931, <https://doi.org/10.1107/S2052520614021192>.
- [15] E.I. Pogoreltsev, I.N. Flerov, A.V. Kartashev, E.V. Bogdanov, N.M. Laptash, Heat capacity, entropy, dielectric properties and  $T$ - $p$  phase diagram of  $(NH_4)_3TiF_7$ , J. Fluor. Chem. 168 (2014) 247–250, <https://doi.org/10.1016/j.jfluchem.2014.10.016>.
- [16] S.V. Mel'nikova, E.I. Pogoreltsev, I.N. Flerov, N.M. Laptash, Unusual sequence of phase transitions in  $(NH_4)_3TiF_7$  detected by optic and calorimetric studies, J. Fluor. Chem. 165 (2014) 14–19, <https://doi.org/10.1016/j.jfluchem.2014.05.016>.
- [17] A.V. Kartashev, M.V. Gorev, E.V. Bogdanov, I.N. Flerov, N.M. Laptash, Thermal properties and phase transition in fluoride,  $(NH_4)_3SnF_7$ , J. Solid State Chem. 327 (2016) 269–273, <https://doi.org/10.1016/j.jssc.2016.02.027>.
- [18] A.X.S. Bruker, TOPAS V4: General Profile and Structure Analysis Software for Powder Diffraction Data. – User's Manual, Bruker AXS, Karlsruhe, Germany, 2008.
- [19] L.D. Landau, E.M. Lifshitz, Statistical Physic, Elsevier, 2013.
- [20] I.N. Flerov, M.V. Gorev, S.V. Mel'nikova, S.V. Misyul, V.N. Voronov, K. S. Aleksandrov, A. Tressaud, J. Grannec, J.-P. Shaminad, L. Rabardel, H. Gengar, Study of the successive phase reansitions  $Fm-3m \leftrightarrow I4/m \leftrightarrow P2_1/n$  in  $Rb_2KInF_6$  and  $Rb_2KLuF_8$  elpasolites, Solid State Phys. 34 (1992) 3493–3500.